ENABLING BIOMIMETIC MORPHING UAVS

Yohanna Hanna[1], Geoffrey Spedding[1], Roy Kornbluh[2], Gordon Kirkwood[2], Mark West[3] and Jay Kudva[3]

[1] Department of Aerospace and Mechanical Engineering, University of Southern California, Los Angeles, CA 90089-1191, {yhanna@usc.edu, geoff@usc.edu} ame.usc.edu
[2] SRI International, Menlo Park, CA 94025-3493, {roy.kornbluh@sri.com, Gordon.kirkwood@sri.com} www.sri.com
[3] NextGen Aeronautics, 2780 Skypark Dr., Torrance CA 90505, {mwest@nextgenaero.com, jkudva@nextgenaero.com}, www.nextgenaero.com

Keywords: Biomimetic, Electrolaminates, Telescopic wings, Morphing

ABSTRACT

We are executing a program to design and test a practical, morphing wing aircraft. Though certain aspects of the design are biomimetic, others are not. We mix and match these elements to provide a demonstrator aircraft that shows, in the simplest way, what benefits accrue from basic morphing changes. The simplest morphing concept is to change the wing area and aspect ratio. The basic contributions of these parameters are well established in classical flight mechanics. We combine this variation with a tail-body configuration that is suggested by previous and continuing work on the vehicle-level flight efficiency of tailless aircraft, or rather where a standard tail geometry is replaced by a trailing edge flap that converts the cargo-carrying body into a lifting body. Finally, the practical shape-changing is enabled by the use of novel electrolaminate materials that can quickly change stiffness at varying positions/postures.

1 INTRODUCTION

The basic idea of a morphing aircraft where the vehicle changes its shape (or more generally its state) to optimally perform in multiple flight segments holds the promise of achieving unprecedented levels of efficiency and enable missions which cannot currently be performed by a single aircraft. Basic shape changes achieved by flaps and other control surfaces, provide capabilities such as efficient landing/take-off over reasonable distances and in maneuvering. While variable-sweep wings (F-111, B-1, F-14) represent operational state-of-the-art, large morphing changes in wing configuration parameters such as area, chord, span, and camber have been largely limited to R&D efforts. The most representative in this area are the DARPA/AFRL Morphing Aircraft Structures programs [1-3], executed by NextGen, Lockheed Martin, and others, which focus on large UAVs. In contrast, if we look at smaller aircraft – of the order of tens of pounds (comparable to AV Raven/Puma) – we may take inspiration from similarly-sized birds to significantly increase efficiency and functionality. By continuously varying wing shape, birds can efficiently handle different flight conditions.

Here we describe elements of a program to design and test a practical, morphing wing aircraft. The overall goal of the program is to develop UAVs capable of adaptively changing aerodynamic configuration using novel active materials, thereby overcoming limitations of prior attempts at implementing practical morphing vehicles. For instance, biomimetic concepts can be exploited to fly in urban and indoor environments, which is difficult to do with current generation small UAVs (SUAVs). Specifically, the focus is to develop novel designs enabled by using ultra-lightweight, multi-functional electrolaminate technology developed by SRI.

2 PRELIMINARY ANALYSIS AND THE BENEFITS OF MORPHING

Simple flight mechanics can demonstrate the potential for morphing. These analyses have been implemented with a Matlab-based GUI tool, so parameter sweeps can be efficiently accomplished. Fig. 1a shows the lift:drag ratio, L/D, as a function of flight speed, U, for a family of curves for various

wing spans (b) (and corresponding wing planform areas, S). These are for a specific aircraft weight, fuselage and tail geometry, engine, and airfoil cross-section. The important point is that for a given aircraft configuration with fixed wing geometry, L/D is maximum at a specific speed; all other parameters held constant, and with increasing span, this speed decreases while the absolute value of $(L/D)_{max}$ increases, asymptotically approaching the value for a flying wing. Hence, to fly efficiently at a wide range of speeds, the wing area needs to continuously change (along the pareto front line in Fig. 1a) and have an aircraft configuration as close to a flying wing as possible.

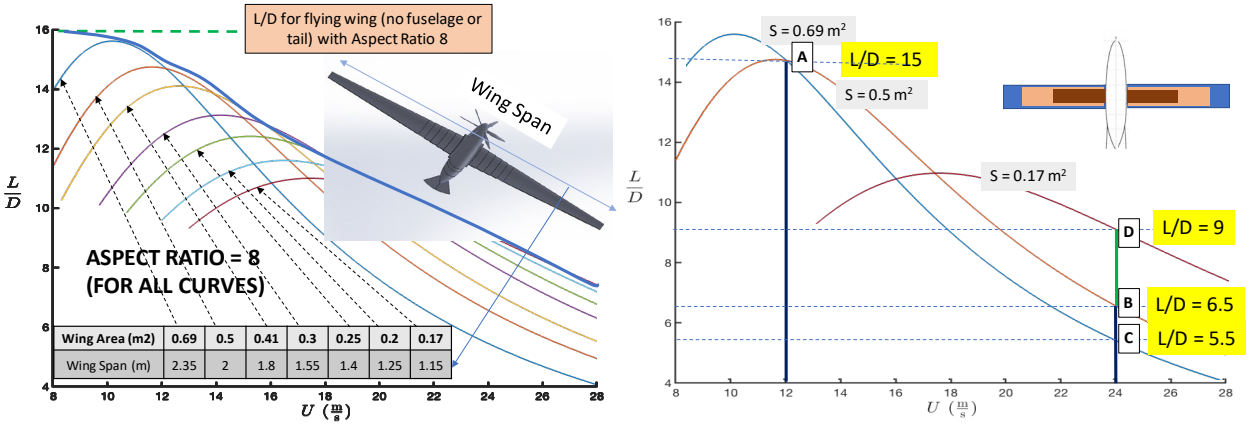

Figure 1: (a) $L/D(U)$ at fixed AR for different planform areas, S; (b) 3 curves with numerical examples

Fig. 1b demonstrates the fundamental benefit of morphing. We start with a wing of area $S_0 = 0.5$ m^2, for which $(L/D)_{max} = 15$ at a speed, $U_0 = 12$ m/s (point A in Fig. 1b). With increasing U, either increasing or decreasing S does not improve (and in fact worsens) L/D. If we now fly at twice the speed, $U_2 = 24$ m/s (Point B), L/D drops to 6.5. For a larger wing with area $S_2 = 0.69$ m^2 (which also has $L/D = 15$ at U_0), L/D at U_2 would be even lower, = 5.5 (Point C). On the other hand, if we reduce the wing area to say, $S_1 = 0.17$ m^2, L/D increases to 9 (Point D), still lower than the value of 15 at U_0 but considerably higher than the value of 6.5 for the original, fixed geometry configuration. This increase is the benefit of morphing – *it reduces the aerodynamic penalty to be paid at non-optimal design points.* This benefit needs to be balanced against the structural weight penalty and mechanical complexity of a morphing wing design and associated mechanisms.

3 FLIGHT VEHICLE DESIGN

Figures 2 – 5 show CAD drawings of the morphing vehicle design. The wing span is 2.4 m when fully extended and 1.2 m when fully retracted; the design allows for continuous span change. When retracted, the inner segments nest and the outer wing-half becomes the entire exposed wing. This approach also allows various configurations for this section including sweep, twist, and winglets. (Fig. 5).

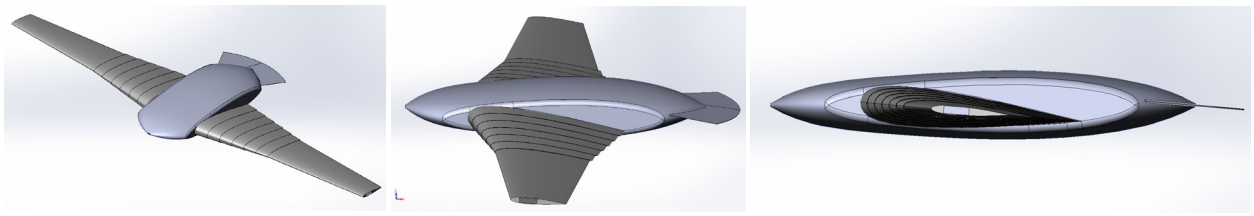

Figure 2: Multiple Views of Morphing UAV

The body itself has a cross-section as proposed by Myring [5]. Although the design Re is 10^7, numerical estimates have been made of the flow fields and forces on such a body-tail configuration [6] so these contributions to the whole aircraft can be considered at least somewhat known.

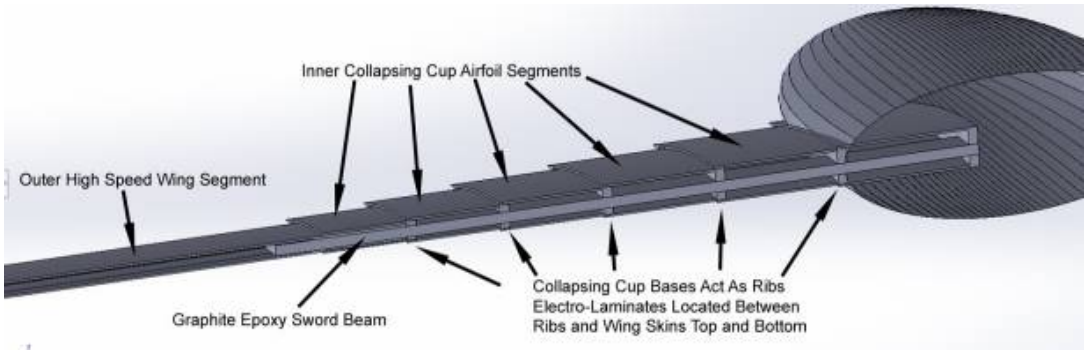

Figure 3: 7-Segment wing cutaway at full extension

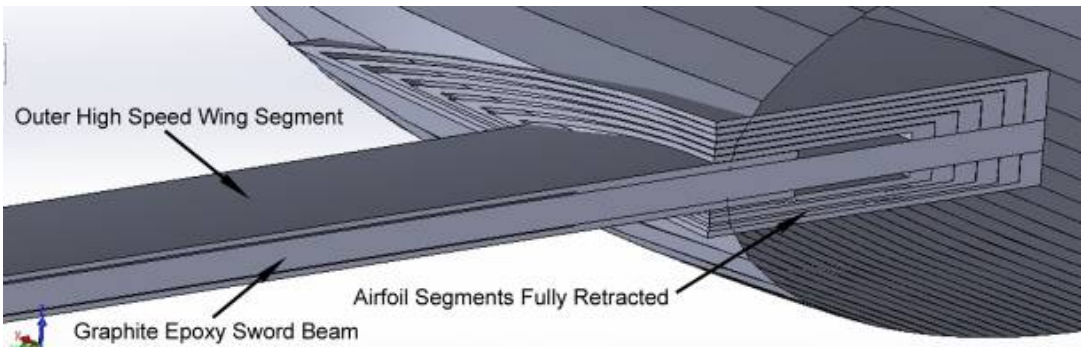

Figure 4: 7-Segment wing cutaway on full retraction

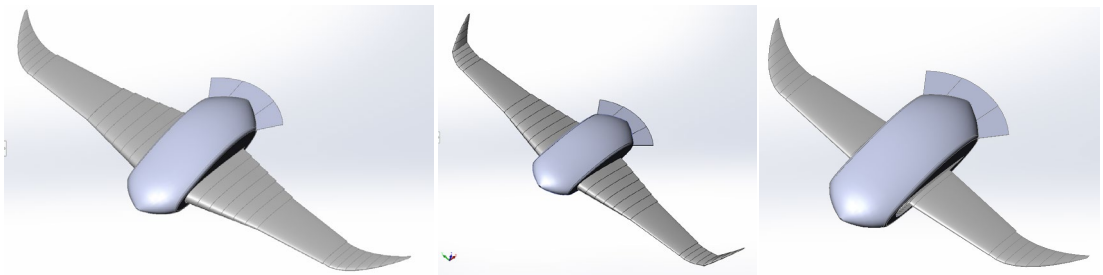

Figure 5: Extended and retracted wings with scimitar winglets and splayed tail feathers

The tail area can be varied continuously for both vehicle control and stability for different wing spans. This variation is achieved using overlapping tail feathers and electrolaminate technology. The configuration is new and must be tested for stability and control as the control laws will be unconventional. These tests continue today with the overall goal of a flying vehicle. Other than the variable wingspan, two features of the configuration in Fig. 5 differ substantially from a standard design. First the body is short (in the flightwise direction), with low fineness ratio (fuselage length, l, to width, d). l/d of 5-7 are actually superior for a body designed for low drag per unit volume, but the pitching moment arm from tail control actions will be low and with low damping. The second feature is the variable deflection and splaying tail, which is now responsible for pitch and roll stability and control. It remains to be tested how these controls must be mixed to set trim and maneuver from that.

The design is being refined based on lab and wind tunnel tests as well as higher-fidelity analyses (aerodynamic, structural and controls).

4 WIND TUNNEL TESTING

A telescoped wing design leads to a planform that has stepwise discontinuities (Fig. 6), whose aerodynamic consequences may be subtle or unexpected, though some earlier literature results suggest that the effects may be small [7] and controllable [8,9].

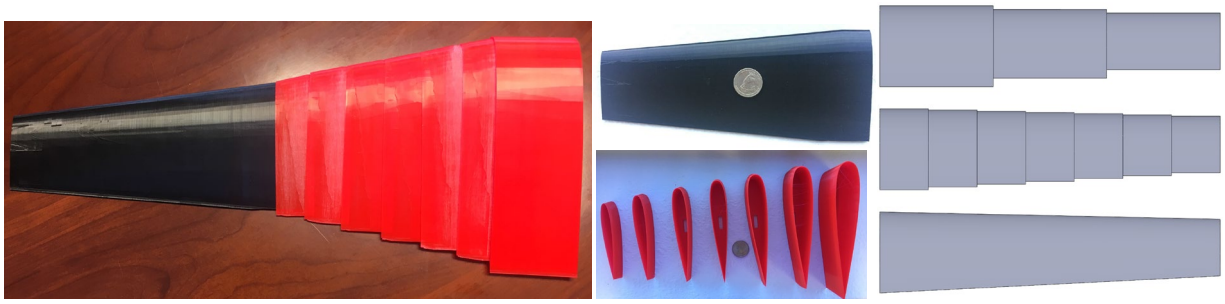

Figure 6: 30% scale 3D printed wing, with outer section (middle top) and inner segments (middle bottom), and the 3 wind tunnel model planforms.

Wind tunnel experiments were conducted on three NACA 0012 profile wings with S=714 cm^2, b=42 cm, c_r= 10 cm, and c_t=7 cm, but with varying number of sections, as seen in Fig. 6. Each section of the stepped wing had a constant local b and c. The 30%c chordwise locations, thickest point of the profile, were aligned for all sections. A simple tapered wing was used as a baseline configuration. Experiments were conducted at Re=73,700 based on the mean aerodynamic chord. Boundary layer trips were placed at 10%c on the suction side to minimize low Re effects. The basic aerodynamic test results are shown in Fig. 7.

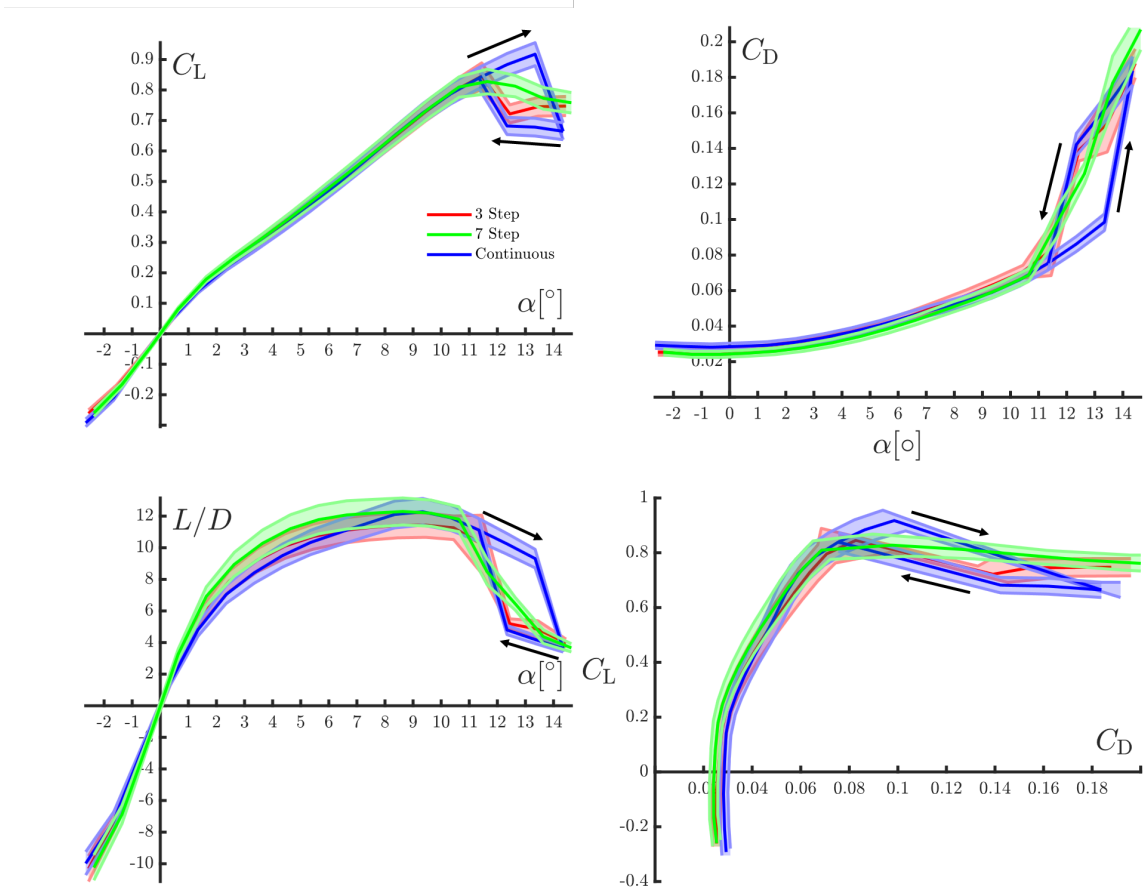

Figure 7: The lift and drag on smooth and stepped wings, AR = 2.5.

The $C_L(\alpha)$ curves are slightly nonlinear at small α, even though the wing models all had boundary layer trips. Up until stall, there is no measurable difference in either C_L or C_D. The small differences that are not themselves distinguishable do combine to yield a slightly flatter plateau in $L/D(\alpha)$. There is some indication that the stepped-wing profiles lack the hysteresis of the smooth wing. All of these properties seem to make the stepped wing a preferred shape. The mechanism for the stable aerodynamics of the stepped wings close to stall may be related to the influence of streamwise vortices shed at the steps. Their effect may change in a crossflow, and to test this possibility the same wings were measured with a 10° sweep (and no other geometry change) so the mean flow runs across the chordwise steps that are no longer aligned with the freestream. A single example is given in Fig. 8.

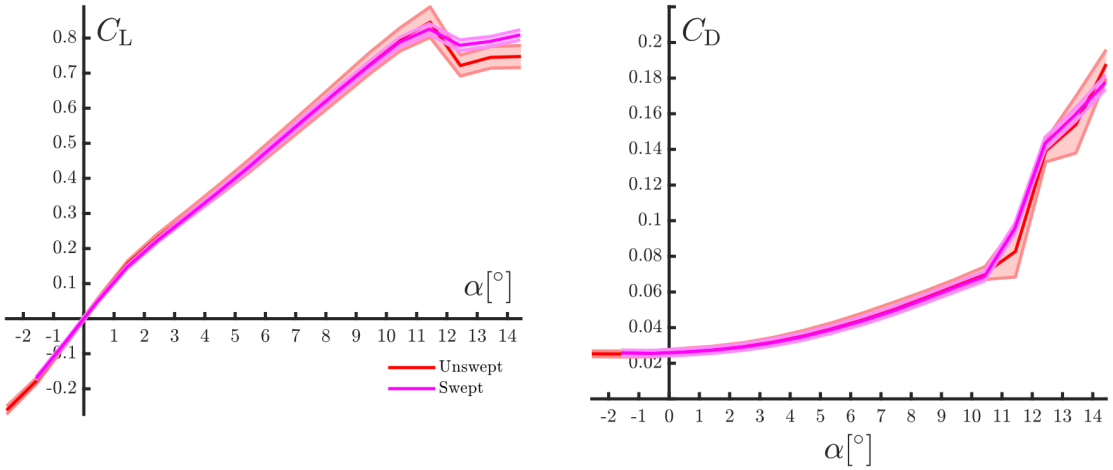

Figure 8: Lift and drag for swept (magenta) and unswept (red) wings. 3-step geometry.

There is no measurable influence of sweep, and at high α, the swept case is, if anything, more robust in stall. The same result was obtained for the 7-step case.

The tests described thus far have been static tests, and it is essential to know the dynamic response for all moving or morphing parts. In particular, the tail assembly will play a critical role, since it is charged with trim and pitch control. A controllable tail assembly was constructed and tested as follows.

The tail is comprised of three rigid flat elements (referred to as “feathers”). One feather is fixed in a central position. The movable feathers are driven by two independent servos that control splaying. With two servos, asymmetric splaying for roll and yaw control is possible. An additional servo controls the pitch of the entire set of three feathers. At each position, the splaying position is locked through the use of electrolaminates. Fig. 9 shows the tail assembly at different splaying configurations. The tail assembly was built into a custom molded carbon-fiber composite shell.

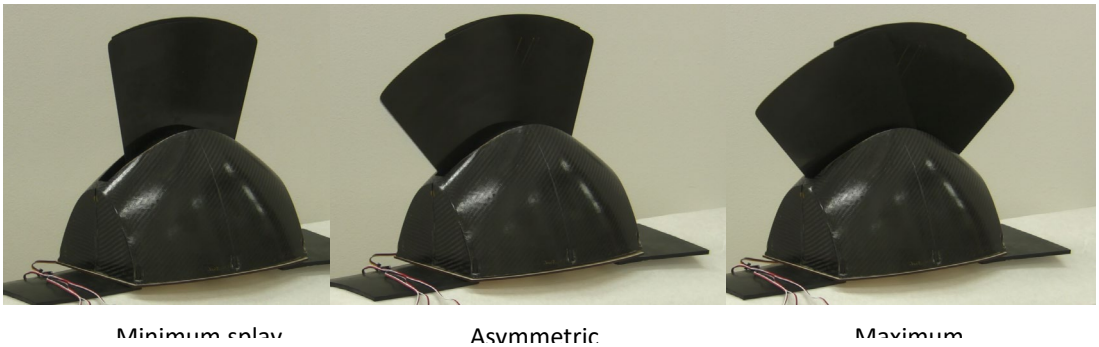

Figure 9: Final tail feather assembly demonstrating a range of tail feather motions

The central and two side tail components (referred to as feathers) are locked and unlocked with respect to each other through application of a low current, high voltage to the circular clutch plates (Fig. 10). The electrolaminate clutch offers several advantages. The locking stiffens the positioning of the feathers, and it can also save energy by not requiring a stall current to be maintained on the backdrivable servo. The locking can also protect the servos from back loads that might result from high loads upon landing or other impact. Such clutches also have the potential to allow for multiplexing of actuation for control of large numbers of degrees-of-freedom. In the present design such multiplexing is not warranted since we have only two moveable feathers. The multiplexing approach has been implemented in robotic hands, for example, where a single servomotor can control multiple joints [Aukes et al. 2014].

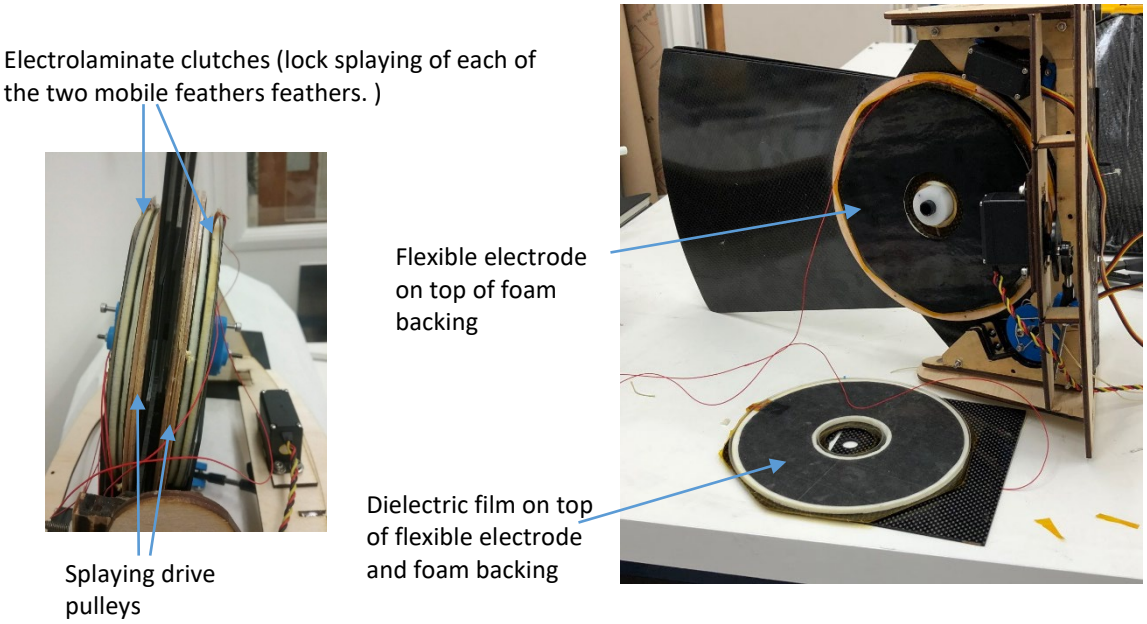

Figure 10: Structure and location of the electrostatic clutches. Clamping connects the movable feathers to the central fixed feather.

Electrolaminates refer to the use of electrostatic forces to control the sliding of layers in a stacked structure. In this case, electrostatic forces are generated between the rotating clutch plates. An electrostatic clutch, compared to other types of clutches such as electromagnetic can be extremely thin and light since the clutch plates themselves apply the needed clamping forces. No additional actuator is needed. Electrostatic clutches have been proposed previously [Fitch 1957], and electrostatic clamping is already widely used in applications such as electronic wafer handling. The innovation here is that the clutch plates include some flexibility in the out-of-plane direction to allow for more intimate contact between the plates. This contact allows for much greater clamping forces. The clutches can clamp with more than 5 Nm of locking torque.

In addition to the rotary clutches, we continue to develop the electrolaminate technology for use in the bending stiffness (and shape locking) of airfoils, and though the current focus has been on the tail feathers, the same strategy can be applied to control surfaces and the airfoil section itself on the outer wing section.

5 NEXT STEPS

The first order benefit in a morphing program can be realised when and if significant changes in wing area can be achieved. Bio-flyers do this through very extensive folding and overlapping of wing

elements, but for a robust engineered solution a telescoped wing can do the same thing. The mechanical complexity is reduced and the variation of mean aerodynamic center with span can be more easily controlled. A possible disadvantage is in the aerodynamic effect of the stepwise discontinuities in wing chord (and height). Careful tests are summarised here and show that there is no substantial effect, even for crudely-varying, 3-step planforms, and that the high angle of attack characteristics may even be improved. The biomimetic components lie in the moving tail parts whose position is locked and unlocked in novel electrolaminate assemblies. Early results are promising for their deployment in flight.

ACKNOWLEDGEMENTS

The authors are most grateful for the support of [insert contract # here] administered and overseen by Dr Les Lee. We are also very grateful to USC undergraduates Haya Helmy, Patrick Valadez, and Stephen Douglass for their assistance in the printing and testing of wind tunnel models.

REFERENCES

[1] Kudva, J., et al., "Design of the NextGen Morphing Wing Wind Tunnel Model," AIAA SDM Conference, AIAA-2007-1730, AIAA, Honolulu, HI, 2007.

[2] Joshi, S., Jha, A., Rodrian, J., Alphenaar, R., and Szema, K., "Design of the NextGen Morphing Wing Wind Tunnel Model," AIAA SDM Conference, AIAA-2007-1731, AIAA, Honolulu, HI, 2007.

[3] Hebert, C., West, M., and Cannon, B., "Actuation System Design, Fabrication, and Testing for a Morphing Wing Structure," AIAA SDM Conference, AIAA-2007-1732, AIAA, Honolulu, HI, 2007.

[4] DARPA-BAA-15-16 "Fast Lightweight Autonomy (FLA)," Defense Sciences Office, 22 Dec 2014.

[5] Myring, D. F., "A theoretical study of the effects of body shape and Mach number on the drag of bodies of revolution in subcritical axisymmetric flow," Royal Aircraft Establishment TR 8100, 1981

[6] Smith L, Craig KJ, Meyer JP & Spedding GR 2018 Numerical investigation of the aerodynamic performance for an alternative wing-body-tail configuration. *J. Aircraft* DOI: 10.2514/1.C034595, 2018

[7] JE Blondeau and DJ Pines, Design and testing of a pneumatic telescopic wing for unmanned aerial vehicles, *J. Aircraft* **44**, 2007, pp 1088-1099 (doi: 10.2514/1.22205).

[8] JJ Henry, JE Blondeau and DJ Pines, Stability analysis for UAVs with a variable aspect ratio wing, *46th AIAA/ASME/AHS/ASC Structures, Structural Dynamics & Materials Conference*, AIAA 2005-2044

[9?] T Yue, X Zhang, L Wang and J Ai, Flight dynamic modeling and control for a telescopic wing morphing aircraft via asymmetric wing morphing, *Aerosp. Sci. Tech.* **70**, 2017, pp 328-338.

[10] Aukes, D.M.C., B. Heyneman, J. Ulmen, H. Stuart, M. R. Cutkosky, S. Kim, P. Garcia, and A. Edsinger, "Design and testing of a selectively compliant underactuated hand," *The International Journal of Robotics Research*, vol. 33, no. 5 (April), 2014, pp. 721–735

[11] Fitch, Clyde J.. "Development of the Electrostatic Clutch." *IBM Journal of Research and Development*, 1 (1957), pp: 49-56.